

# AUBE '01

12TH INTERNATIONAL  
CONFERENCE <sup>ON</sup> AUTOMATIC  
FIRE DETECTION

March 25 - 28, 2001  
National Institute Of Standards and Technology  
Gaithersburg, Maryland U.S.A.

## PROCEEDINGS

Editors: Kellie Beall, William Grosshandler and Heinz Luck



**NIST**  
National Institute of Standards and Technology  
Technology Administration, U.S. Department of Commerce

Thomas Cleary, Michelle Donnelly, George Mulholland, and Bakhtier Farouk\*  
Building and Fire Research Laboratory, Natl Inst of Stds and Tech Gaithersburg, MD  
20899, USA

\*Mechanical Engineering and Mechanics Department, Drexel University  
Philadelphia, PA 19104, USA

## **Fire Detector Performance Predictions in a Simulated Multi-room Configuration**

### **1. Introduction**

Modeling fire detector performance requires detailed information on the environment surrounding the detector, the species transport (heat, particulate smoke, and gases) from the surrounding to the sensing surface or volume, and the sensor response. The details of the environment surrounding a detector can be gathered from full-scale fire experiments, however, that approach affords very little flexibility. One **may** be able to find information gathered from standard fire sensitivity tests or other single-room fire tests, but not for complex configurations. In a performance-based approach, an ideal situation is one where modeling replaces full-scale experiments wherever possible. Luck and Sievert [1] refer to the environment surrounding the detector **as** the "outer world" , where all aspects important for fire detection must be modeled including both fire and non-fire conditions. Once the detector environment is known, the species transport to a detector's sensing surface or volume and its response can be modeled if sufficient detailed information on a particular detector exists. An alternative approach is to perform detector exposure experiments in the fire emulator/detector evaluator to ascertain sensor responses for modeled, realistic fire scenarios.

### **2. Modeling Detector Fire Environments**

Modeling of detector environments has evolved from the ceiling jet correlations applied to (thermal) detector activation, zone modeling, to more detailed computational fluid dynamics models. Davis [2] has developed a zone fire model "Jet" which has a ceiling jet correlation embedded in the computational algorithm to facilitate better temperature, smoke and species concentrations, and flow conditions at detector locations. The model

formulation has been used in a sensor driven fire model that utilizes thermal and/or smoke sensor outputs to predict fire conditions [3]. Andersson and Holmstedt [4] performed a computational fluid dynamics (CFD) study to predict temperature and smoke light extinction at a detector location in a simulated EN 54 part 9 fire sensitivity test. Davis *et al.* [5] used CFD computations to study complex ceiling geometry effects on detector activation. Cleary *et al.* [6] used the Fire Dynamics Simulator, (FDS; a computational fluid dynamics fire model based on large eddy simulation technique, developed by NIST [7]) to predict the smoke, thermal and flow environment at a detector located in a simulated EN 54 part 9 test room subjected to test fire 4.

Here, the fire model FDS was used to predict the fire environment at multiple detector locations in a three room suite. Specifically, FDS was used to compute velocity, temperature, smoke and CO gas concentrations at detector locations in each room of a simulated fire located in one of the three rooms. A diagram of the room layout, fire and detector locations is shown in Figure 1. Room 1 is the fire room, where the fire source is located at the floor in the center of the room. The ceiling height is 2.90 m and the door openings are 0.91 m wide by 2.44 m high. Supply and return HVAC vents (0.3m wide by 0.9 m high) are located in the walls at a height 0.3 m from the ceiling, and have fixed flows between 0.04 m<sup>3</sup>/s and 0.2 m<sup>3</sup>/s. The return in room 2 acts as an open vent. The ambient temperature was 20 °C and the surfaces were adiabatic (i.e., no heat loss to wall or ceiling). The computational grid spacing was  $x = 150$ ,  $y = 75$ , and  $z = 27$ , for a total of 303,750 cells and a physical grid spacing of 17.2 cm, 20.8 cm, and 10.7 cm for x, y, and z directions respectively.

The simulated fire consisted of a flaming fire that starts out with a heat release rate similar to the EN54 TF4 flaming polyurethane foam mat fire. It transitions to a "medium  $t^2$  fire" after the mat fire reaches its peak output at 200 s (Figure 2). The radiative fraction was set at 0.35 with a heat of combustion fixed at 16 kJ/kg. The smoke and CO yields of 0.03 g smoke/g burned and 0.01g CO/g burned are in the range of what would be expected from a flaming plastics fire. The detector locations represent two separate detector spacings of 9.1 m (30 ft.) for locations 1, 3, 8, and 9, and 6.4 m (21 ft.) for locations 1, 2, 4, 5, 6, 7, 10, 11, and 12. The environment was simulated for 500 s with

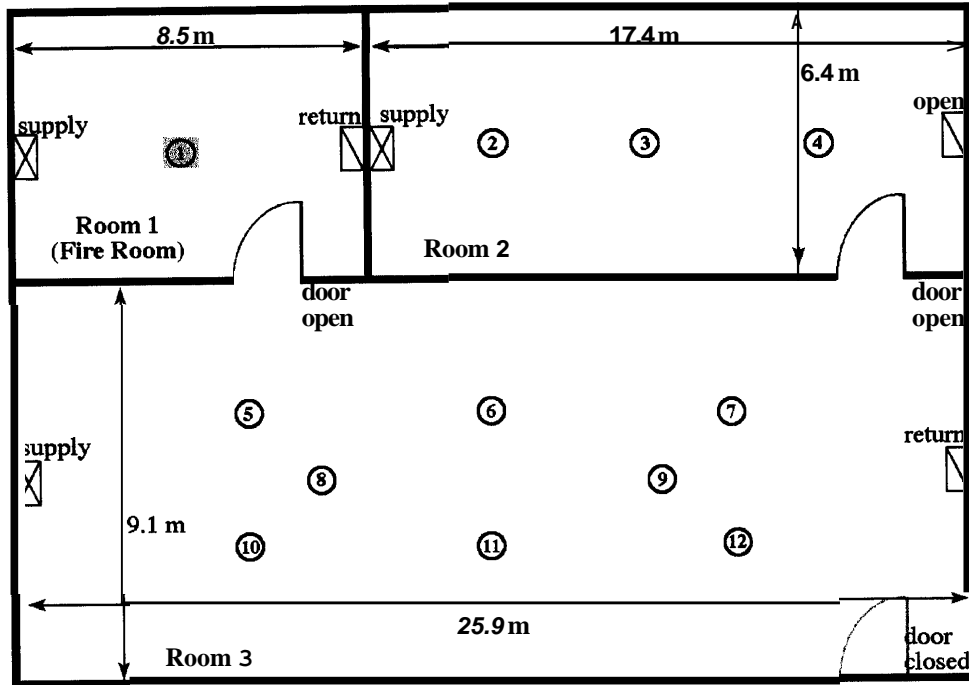


Figure 1. Three room suite layout; circled numbers are detector locations.

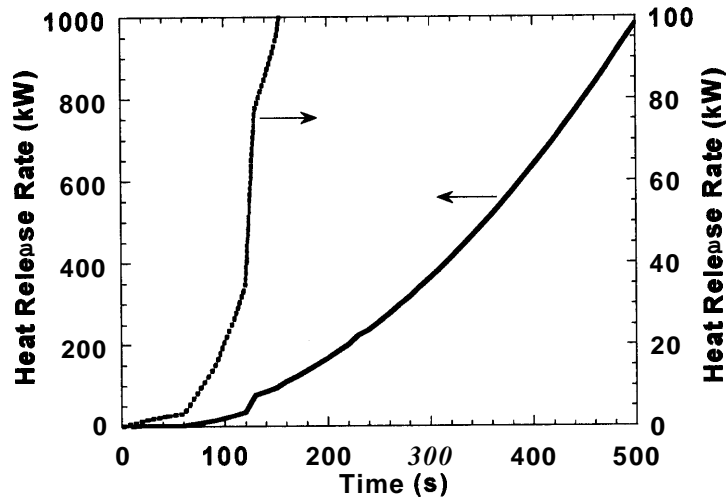


Figure 2. Heat release rate curve used in FDS computation.

the temperature, smoke and CO concentrations, and the  $x$  and  $y$  flow velocity vectors recorded at each detector location (i.e., the computational grid at the ceiling which encompasses a typical detector's vertical position). The  $x$  and  $y$  velocity vectors were used to compute the scalar horizontal flow speed as a function of time at each detector

location. The smoke concentration was converted into an extinction coefficient by multiplying the smoke concentration in grams per m<sup>3</sup> by a specific extinction coefficient for soot of 8.7 m<sup>2</sup>/g [8].

Figures 3 and 4 show the temperature, flow speed, CO volume fraction, and smoke extinction coefficient computed at detector location 1 (L1) in the fire room. In Figure 3, the temperature rise curve has the same shape as the heat release rate curve. The plume centerline temperature at the ceiling was computed from Heskestad's strong plume correlation at ambient background temperature of 20 °C [9];  $\Delta T = 25 Q_c^{2/3} z^{-5/3}$ , where  $\Delta T$  is the excess temperature (°C),  $Q_c$  is the convective heat release rate, and  $z$  is the height of ceiling from the fuel source. The fact that the correlation predicts higher ceiling temperatures early may be due to the course grid size used in the FDS calculation and the fact that the plume correlation was developed from steady-state fires. The under-prediction later in the computation is due to the fact that the correlation is valid for unconfined plumes, and the effects of entrainment of hot layer gases is not accounted for. The horizontal flow speed is somewhat vague since the plume velocity is turning

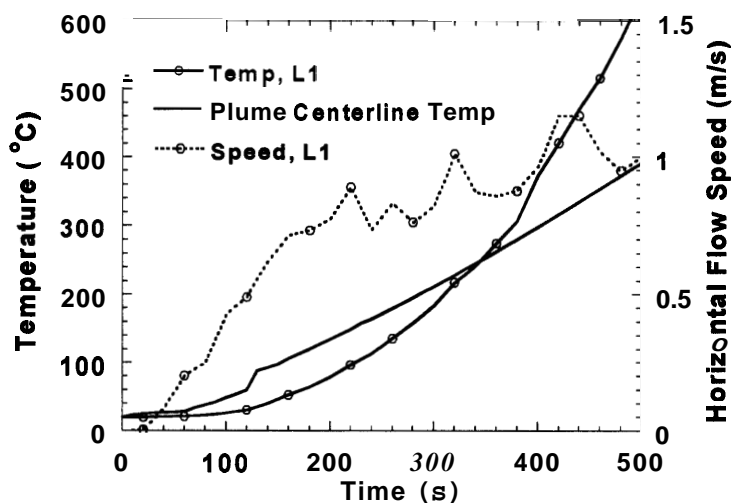


Figure 3. Temperature and flow speed at detector location 1 in the fire room.

from mostly vertical to horizontal directly above the plume. In Figure 4, the CO volume fraction gradually rises (noticeably starting at 60 s) to a peak volume fraction greater than  $500 \times 10^{-6}$  at the end of the simulation time. The extinction coefficient started

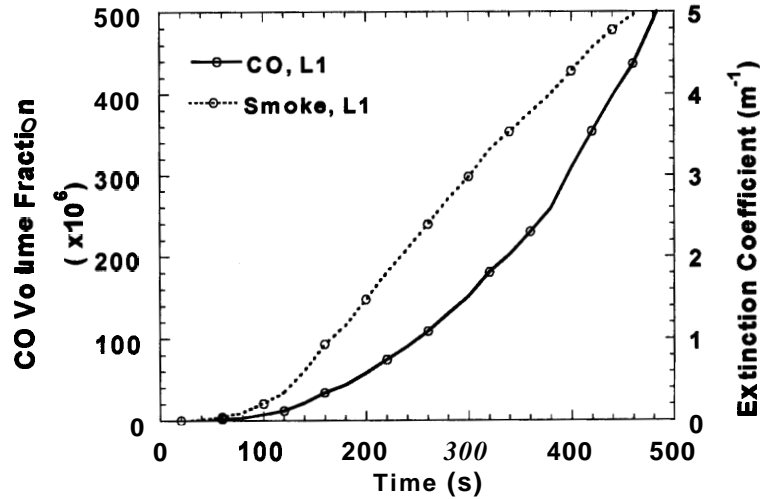


Figure 4. CO volume fraction and smoke extinction coefficient at detector location 1.

to rise at 60 s and continued to rise above  $5 m^{-1}$  by the end of the simulation. For comparison, an extinction coefficient of  $0.13 m^{-1}$  is equivalent to a smoke obscuration of 4 % per 0.3 m (1 ft).

Figures 5 and 6 show the temperature, flow speed, CO volume fraction and extinction coefficient values computed at detector locations 5, 8, and 10. These locations were grouped together due to their proximity to one another and to the door opening from

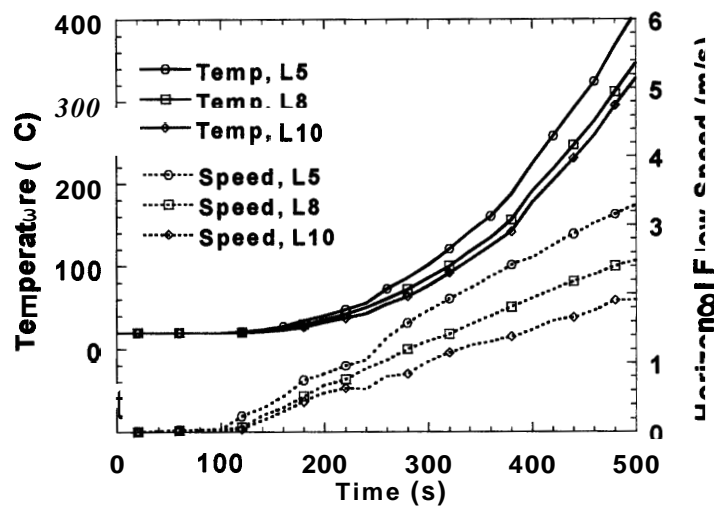


Figure 5. Temperature and flow speed at detector locations 5, 8, and 10 in room 3.

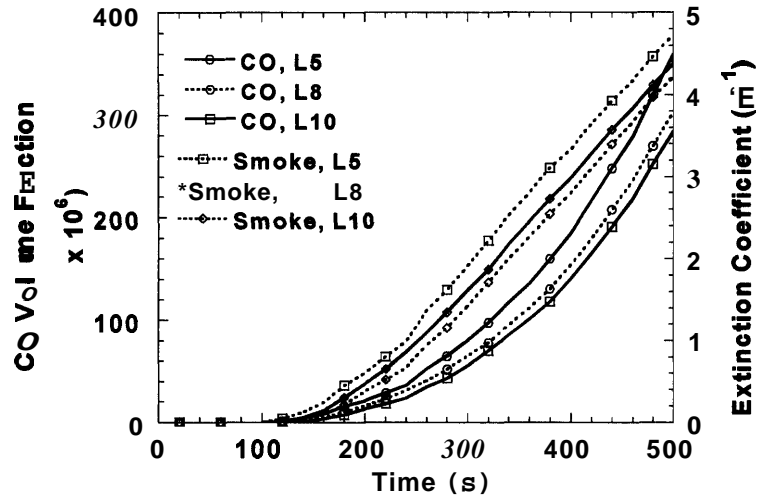


Figure 6. CO volume fraction and smoke extinction coefficient at locations 5, 8, and 10.

room 1. In Figure 5, note that the flow speeds reach levels of over **0.8 m/s** before temperatures rise by **25 °C**, and peak between **1.9 m/s**, **2.5 m/s**, and **3.3 m/s** for locations **5**, **8**, and **10** respectively. These flow speeds are created from the jet issuing from the doorway. In Figure 6, the CO volume fraction curves look similar to the CO volume fraction in room 1 except that the initial rise started at **120 s** and the peak volume fractions were lower than at location 1. Smoke extinction followed a similar path compared to location 1, however, initial rise was delayed by 40 s to **80 s**.

Figures 7 and 8 show the computed values at detector locations **6**, **7**, **9**, **11**, and **12**. Again, these were grouped due to their proximity. As expected, all computed values begin to rise later than at locations closer to the fire. Except for location **11** after 300 s, the temperatures, flow speeds, CO volume fraction and extinction values are quite similar, however, shifted in time by **20 s** to **60 s**. The flow speed at location **11** continued to rise after 300 s, achieving a speed of **1.5 m/s** at the end of the simulation, which suggests it was seeing the effects of the doorway jet more directly than the locations **6**, **7**, **9**, and **12**.

Figures 9 and 10 show the computed values at detector locations **2**, **3**, and **4**, all located in room **2**, and the furthest from the fire source. All computed values began to rise

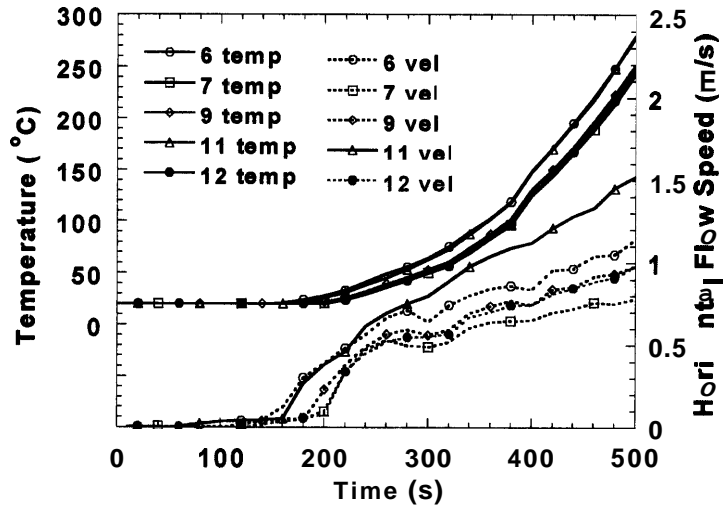


Figure 7. Temperature and flow speed at locations 6, 7, 9, 11, and 12 in room 3.

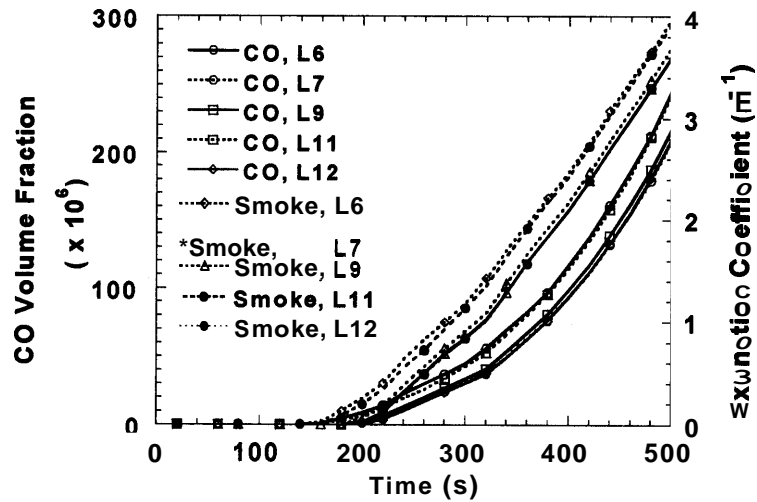


Figure 8. CO volume fraction and extinction coefficient at locations 6, 7, 9, 11, and 12.

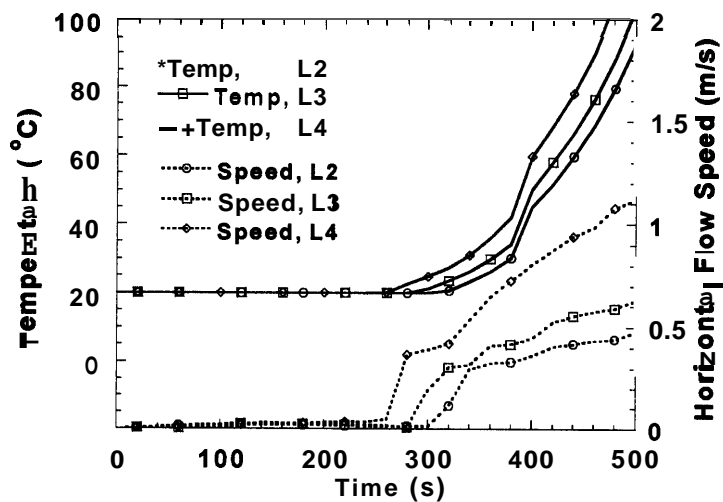


Figure 9. Temperature and flow speed at locations 2, 3, and 4 in room 2.

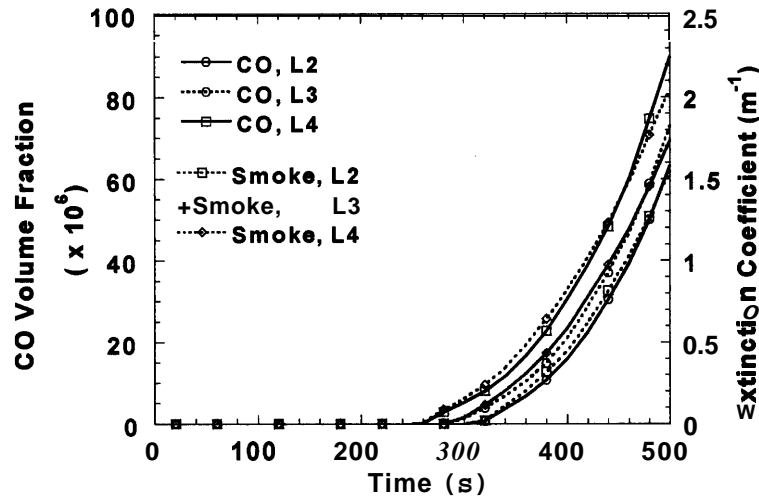


Figure 10. CO volume fraction and extinction coefficient at locations 2, 3, and 4.

260 s and 320 s. The maximum speed at location 4 was nearly twice as large as the maximum at location 3, owing again to its relative position to the doorway opening and the jet issuing from room 3.

### 3. Fire Emulator/Detector Evaluator Tests

The fire emulator/detector evaluator (FEDE) was used to reproduce the computed flow speed, temperature rise, CO and smoke concentrations at select detector locations. The FE/DE is a single-pass wind tunnel where room air is drawn into the opening, and exhausted to a hood at the end of the duct. It was designed specifically to reproduce the environment surrounding a detector during fire or nuisance events [10,11]. In the FEDE, air velocity at the test section can be controlled over a range of flows between **0.02 m/s** to over **2 m/s** by means of a computer-controlled axial blower. The flow is conditioned before it reaches the test section by passing it through a 10 cm long aluminum honeycomb with **5 mm** rectangular openings. The goal was to provide a nominally flat flow profile indicative of what would be expected by a detector in a ceiling jet flow. The flow was monitored at the test section by a bi-directional probe located at the duct centerline. For fixed fan speeds, the flow profile is nearly top-hat with a velocity that fluctuates indicating turbulent flow. Thermal energy is added to the flow by forcing it through a series of **9** annular finned heating elements. Each element is rated at **5 kW** for a total maximum heat input of **45 kW**. Power to the heating elements is controlled by a feedback controller that receives set-point values automatically from a

computer file and compares them to the air temperature exiting the heaters. An air temperature difference between the heater exit and test section locations is due to heat losses to the duct section between those two points. A rate of rise in air temperature of 0.5 °C/s is achievable at the test section, up to maximum temperature of about 80 °C. Air temperature at the test section was recorded with type-K thermocouples.

CO, CO<sub>2</sub>, or other gas blends may be metered into the flow via electronic mass flow controllers. CO, CO<sub>2</sub>, H<sub>2</sub>O, and hydrocarbon gas concentrations are monitored by non-dispersive infrared analyzers. The standard Uncertainty in the CO volume fraction measurement is stated as  $2.5 \times 10^{-6}$ . The ability to control gas concentrations independently benefits both fire and nuisance alarm scenario emulation. For example, both CO and CO<sub>2</sub> may be normally present in ever-changing concentrations in a building due to the external environmental sources such as attached parking garages, or internal sources such as the diurnal CO<sub>2</sub> variation due to occupancy and ventilation levels. The FE/DE can be programmed to reproduce such conditions as part of an evaluation of a fire detector that includes gas detection.

Various smoke and non-combustion aerosols may be introduced into the flow. Here, a propene smoke generator, which provides black soot typical of flaming hydrocarbon or plastics fire smoke, was used. The concentration of smoke in the flow is varied by changing the fuel flow of the burner and opening or closing dampers allowing more or less flow from the burner to enter the duct. Laser light transmission measurements across the duct at the test section were used to calculate the extinction coefficient of the propene soot. A He-Ne laser at 632.8 nm wavelength is the light source, and a stabilizer utilizing a liquid crystal polarizer maintains a nearly constant laser intensity. The beam is split and introduced at two heights: the center of the duct, and 5 cm below the ceiling (here, the extinction measurement from the beam 5 cm below the ceiling was used). Each light beam is reflected off two mirrors inside the duct and directed at a photodetectors placed on the opposite side of where the beam enters the duct. The total path length inside the duct is 1.5 m. The photodetector output voltage is linear with respect to the transmitted light intensity. The standard relative uncertainty due to random fluctuations in output is 0.06% of the measured light transmittance.

A multi-sensor, analog output fire detector was used to record continuous photoelectric and thermal sensor signals during the emulated conditions. These outputs are actually 8 bit numbers from an analog to digital converter. Here, offsets were subtracted so the outputs are zero to start. A CO sensor removed from a residential CO detector was placed in the FEDE test section during the tests and the voltage drop that developed across a resistor placed between the two sensor electrodes was recorded.

The simulated detector environments that were emulated in the FE/DE and reported here are detector location 2 in room 2, and detector location 11 in room 3. The computed values at these locations represent the range of flow speeds and temperature rise achievable in the FEDE. The length of simulation time emulated depends on the flow and temperature rise; the complete 500 s simulation at location 2 was emulated, while only the first 330 s of the simulation at location 11 was emulated. Figure 11 shows the duct velocity and fan settings for two repeats of a test that was designed to emulate conditions developed at location 2. The fan setting was controlled such that the duct velocity matched the simulated flow speed as indicated. Figure 12 shows the duct velocity and fan setting for a test designed to emulate conditions developed at location 11. Again, good agreement between the simulated flow speed and the duct velocity was achieved.

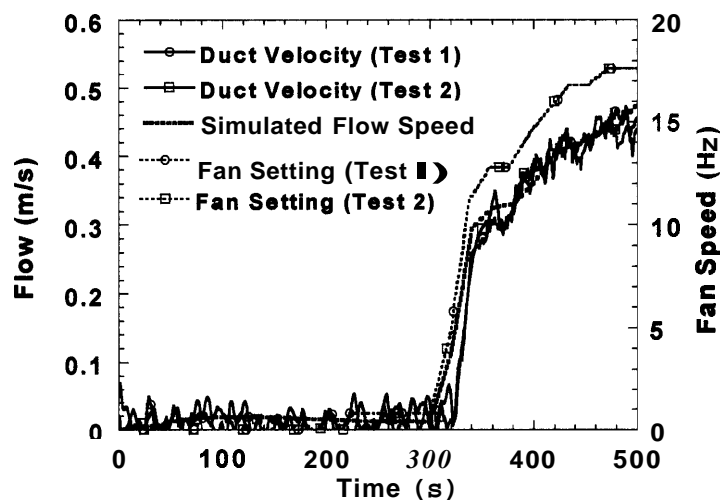


Figure 11. Duct velocity and fan setting for emulated conditions at location 2.

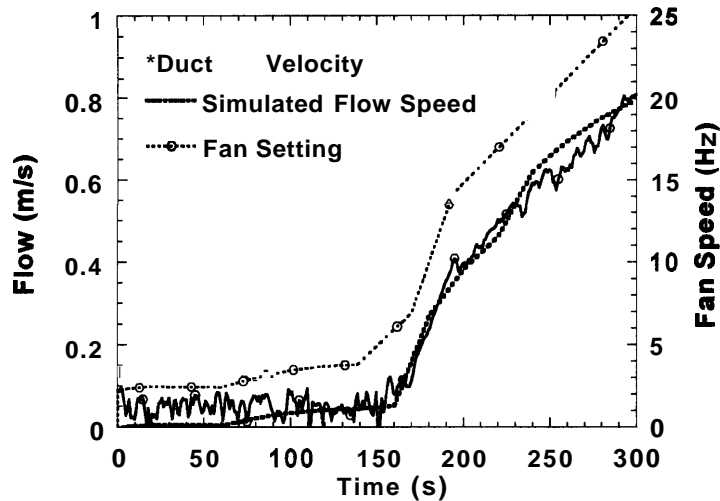


Figure 12. Duct velocity and fan setting for emulated conditions at location 11.

Figure 13 shows the duct air temperature at the test section and the thermal sensor output for repeated tests of the location 2 emulation. The computed temperature and the emulated temperature compare favorably until about 450 s when the emulated temperature starts to deviate from the computed temperature which continued to climb. The thermal sensor lagged the thermocouple temperature due to its response characteristics. Figure 14 shows the duct air temperature and thermal sensor output for the location 11 emulation. Good agreement between the computed temperature and the emulated temperature was maintained until about 330 s when the simulated temperature rose above the operational range of 80 °C of the FE/DE. Note that the lag between the

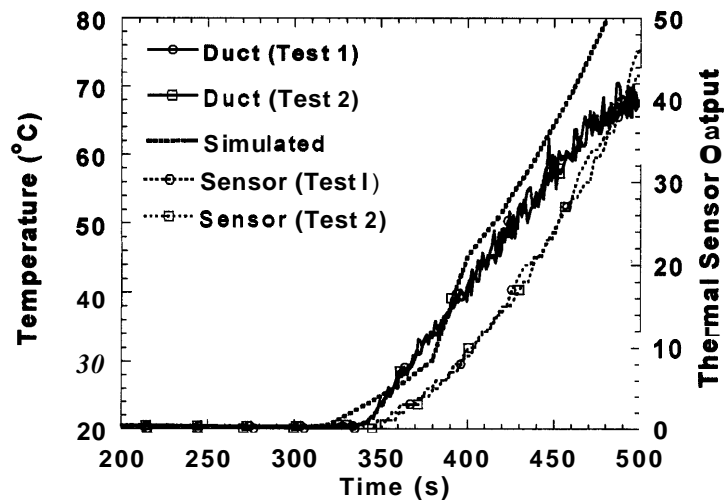


Figure 13. Duct temperature and thermal sensor output for conditions at location 2.

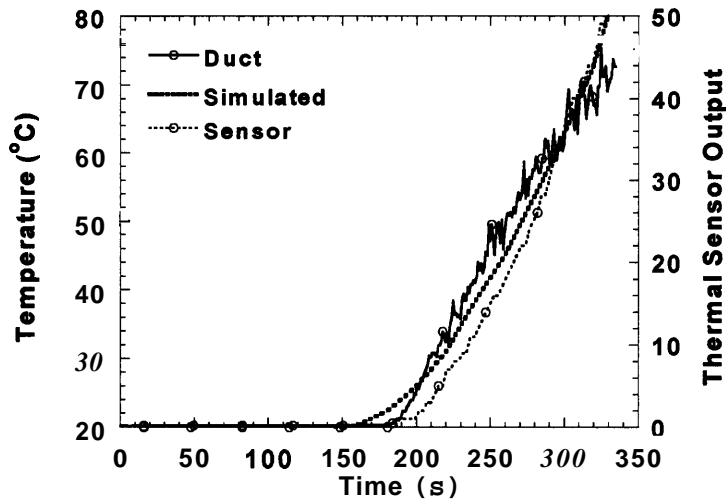


Figure 14. Duct temperature and thermal sensor output for conditions at location 11.

thermal sensor and the thermocouple is less pronounced. This is most-likely due to enhanced convective heat transfer to the thermal sensor in this emulation due to the higher duct flow velocities.

Figures 15 and 16 show the duct CO volume fraction for location 2 and location 11 emulations respectively. The agreement between the duct CO volume fraction and the computed value is not very good. This is due in part to the fact that the lower limit of the selected mass flow controller used to introduce the CO gas into the duct was too high

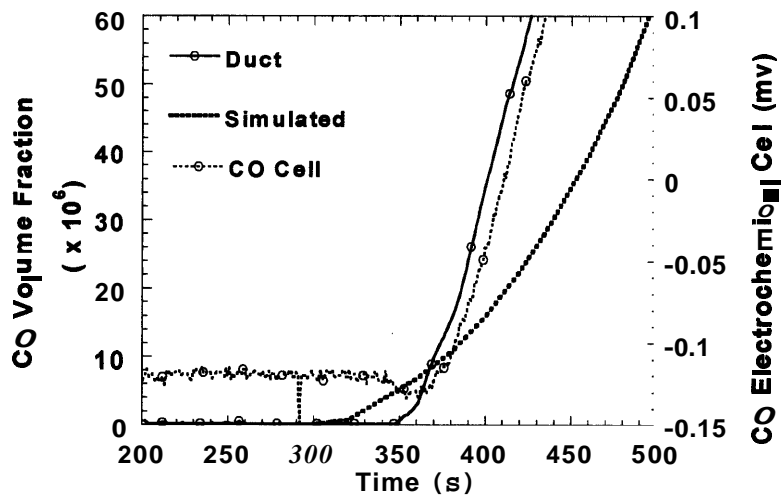


Figure 15. Duct CO volume fraction and CO cell volts for emulated conditions at location 2.

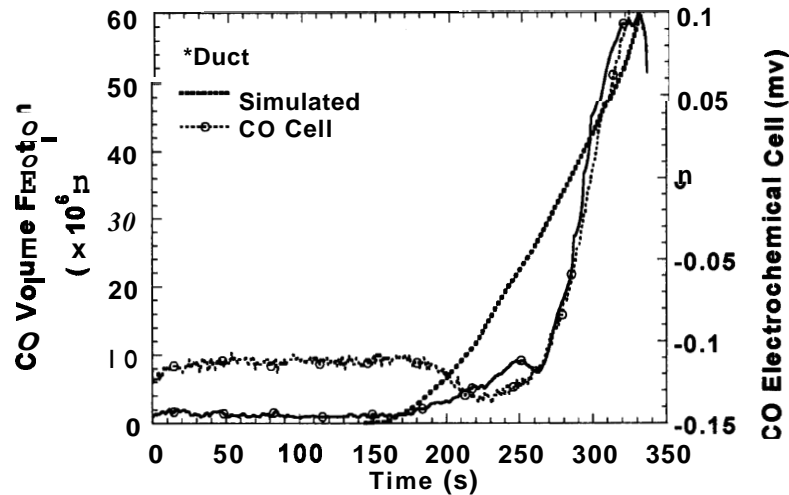


Figure 16. Duct CO volume fraction and CO cell volts for emulated conditions at location 11.

to produce smooth continuous flows of CO needed to achieve the target concentrations. For comparison, the electrochemical cell output is shown, and it compares favorably with the duct CO concentration, with only a short lag time between the curves.

Figures 17 and 18 show the duct extinction coefficient and the computed extinction coefficient for emulation tests of location 2 and 11 respectively. The smoke produced by the propene burner is sufficient to emulate the computed extinction coefficients at

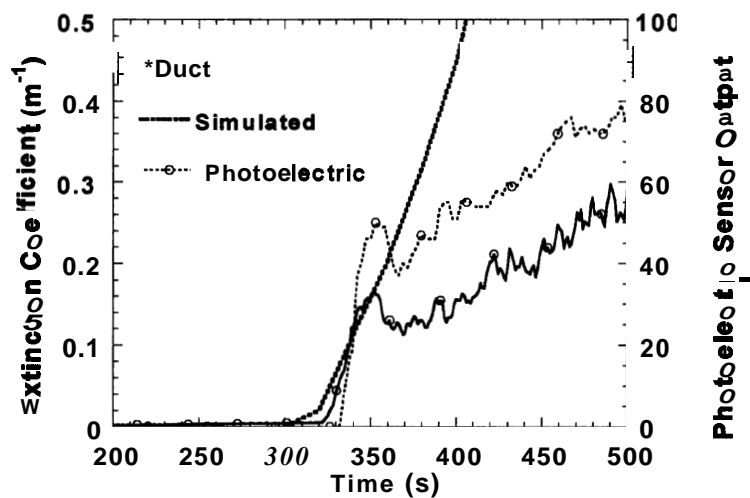


Figure 17. Duct smoke extinction and photoelectric sensor output for emulated conditions at location 2.

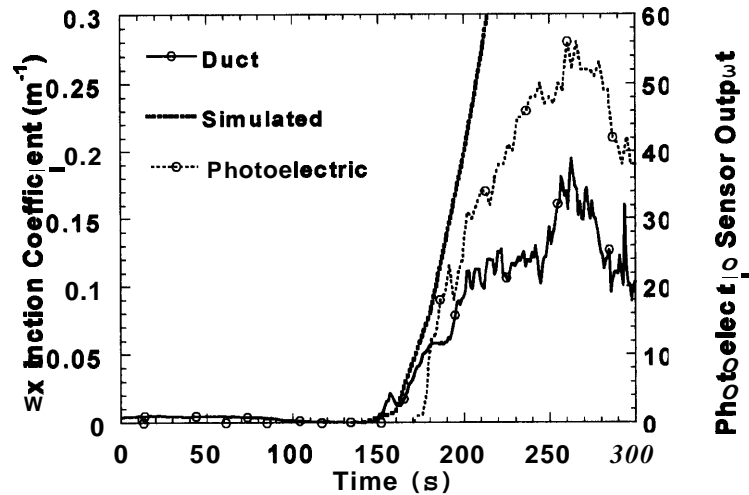


Figure 18. Duct smoke extinction and photoelectric sensor output for emulated conditions at location 11.

each location up to about 0.15 m<sup>-1</sup>. Owing to the ever increasing flow velocity, the smoke production cannot keep up with the simulated smoke build-up. However, a high smoke concentration that produces a large extinction coefficient is not necessarily relevant to detector performance. The photoelectric sensor output tracked the duct extinction coefficient in each emulation. Here, the duct flows are sufficiently high to reduce the smoke entry lag to negligible times.

The particular simulated fire scenario chosen pushed the operation of the FEDE to its limits. Refinement of the FEDE for these emulated conditions is required to overcome the temperature, smoke production, and CO flow limitations.

#### 4. Conclusions

From this work, it is concluded that multi-room fire simulation with the FDS software can yield environmental conditions a detector or sensor may experience during an actual fire. The FDS code computes the smoke, heat, and gaseous species transport needed to predict detector performance. The specific fire scenario simulated here was chosen to produce rapidly changing smoke and gas concentrations, heat, and flow velocities at detector locations. Such a fire test would be quite expensive to perform a single time since the fire room approaches flashover conditions during the computational time. Once a detector environment is specified, the FEDE can reproduce the important

variables of the environment in a repeatable fashion, and actual detectors or sensors can be exposed to the defined environment for performance evaluation.

## 5. References

- [1] Luck, H., and Sievert, U., "Does an Overall Modelling Make any Sense in Automatic Fire Detection?", Proceeding of the 11th International Conference on Automatic Fire Detection "AUBE '99", March 16-18, 1999, Gerhard Mercator University, Duisburg, Germany, Luck, H., Ed., pp 1-9, 1999.
- [2] Davis, W., "The Zone Fire Model Jet: A Model for the Prediction of Detector Activation and Gas Temperatures in the Presence of a Smoke Layer", NISTIR 6324, National Institute of Standards and Technology, Gaithersburg, MD, May, 1999.
- [3] Davis, W., and Forney, G., "A Sensor-Driven Fire Model, Version 1.1", NISTIR in preparation, National Institute of Standards and Technology, Gaithersburg, MD, January, 2001.
- [4] Andersson, p., and Holmstedt, G., "CFD-Modelling Applied to Fire Detection - Validation Studies and Influence of Background Heating," Proceeding of the 10th International Conference on Automatic Fire Detection "AUBE '95, April 4-6, 1995, Gerhard Mercator University, Duisburg, Germany, Luck, H., Ed., pp 429-438, 1995.
- [5] Davis, W., Forney, G., and Bukowski, R., "Developing Detector Siting Rules from Computational Experiments in Spaces with Complex Geometries," Fire Safety Journal, Vol. 29, pp 129-139, 1997.
- [6] Cleary, T., Anderson, M., Averill, J., and Grosshandler, W., "Evaluating Multi-sensor Fire Detectors in the Fire Emulator/Detector Evaluator," Proceedings of the 8th Inter. Conf. on Fire Science and Eng., Interflam '99, Edinburg, Scotland, June 1999.
- [7] McGrattan, K., Baum, H., Rehm, R., Hamins, A., and Forney, G., "Fire Dynamics Simulator - Technical Reference Manual," NISTIR 6467, National Institute of Standards and Technology, Gaithersburg, Maryland, January, 2000.
- [8] Mulholland, G., and Croarkin, C., "Specific Extinction Coefficient of Flame Generated Smoke," Fire and Materials, Vol. 24, pp 227-230, 2000.
- [9] Heskestad, G., "Engineering Relations for Fire Plumes," Fire Safety Journal, Vol. 7, pp. 25-32, 1984.
- [10] Cleary, T., Grosshandler, W., and Chernovsky, A., "Smoke Detector Response to Nuisance Aerosols," Proceeding of the 11th International Conference on Automatic Fire Detection "AUBE '99", March 16-18, 1999, Gerhard Mercator University, Duisburg, Germany, Luck, H., Ed., pp 32-41, 1999.
- [11] Cleary, T., "Performance Characterization of Multi-sensor, Multi-criteria Fire Detectors in the Fire Emulator/Detector Evaluator: Particulate, Thermal, and Gas Sensing Combinations," Proceedings of VdS Conf. on Gas Sensors for Fire Detection, November 15-16, Cologne, Germany, 2000.